DNP NMR studies of crystalline polymer domains by co-polymerisation with nitroxide radical monomers - Supporting Information

Ester Verde-Sesto[a], Nicolas Goujon[b], Haritz Sardon[a], Pauline Ruiz[b], Tan Vu Huynh[b], Fermin Elizalde[a], David Mecerreyes[a,c], Maria Forsyth[b,c] and Luke A. O'Dell[b]*

[a]POLYMAT, University of the Basque Country UPV/EHU, Joxe Mari Korta Center, Avda. Tolosa 7, 20018 Donostia-San Sebastian, Spain.

[b]Institute for Frontier Materials, Deakin University, Geelong, Victoria 3220, Australia

[c] Ikerbasque, Basque Foundation for Science, E-48011 Bilbao, Spain

*Email: luke.odell@deakin.edu.au

Contents

1 - Sample synthesis	**S2**
2 - FTIR	**S4**
3 - DSC	**S5**
4 - SAXS & WAXS	**S8**
5 - DFT	**S10**
6 - DFT-optimised PEO crystal structure	**S13**
7 - PEO domain size measurement	**S14**
8 - Comparison of different linker groups	**S15**
9 - References	**S16**

1 - Sample Preparation

Materials 2,2-Bis(hydroxymethyl)propionic acid (bis-MPA), 2,2-dimethoxypropane, p-toluenesulfonic acid monohydrate (PTSA), phenylhydrazine, Dowex® 50W-X8 200–400 mesh, polyethylene glycol end capped diol (PEG, M_n = 1500 g mol−1), hexamethylene diisocyanate (HDI), 1,8-diazabicyclo[5.4.0]un dec-7-ene (DBU), trifluoromethanesulfonic acid (triflic acid; TfOH), triethylamine (TEA), benzoic acid, 4-hydroxy-2,2,6,6-tetramethylpiperidine 1-oxyl (4-hydroxy-TEMPO; TEMPOL), N,N'-dicyclohexylcarbodiimide (DCC), 4-(dimethylamino)pyridine (DMAP) and silica (High purity grade, 60 Å, 230–400 mesh) were supplied by Aldrich Chemical Corporation. Sodium sulfate anhydrous, dichloromethane (DCM), methanol, ethanol, ethyl acetate (EtOAc), hexane, diethyl ether and acetone were purchased from Acros Organics. Deuterated solvents were bought from Deutero GmbH, Germany. All materials were used as received except for the PEG diol which was dried by azeotropic distillation with toluene for 12 h prior to use.

Monomer and Polymer synthesis

Synthesis of 4-hydroxy-2,2,6,6-tetramethylpiperidine 1-oxyl 3-hydroxy-2-(hydroxymethyl)-2-methylpropanoate (bis-MPA-TEMPO):

The diol containing pendant nitroxide, bis-MPA-TEMPO, was synthesized by following the procedure previously described by Garmendia *et al*. (Ref: Polym. Chem., 2017, 8, 2693-2701) The ^{1}H NMR spectrum was compared against the reported literature and found to be identical.

General procedure for the synthesis of poly(MPA-TEMPO-HDI-PEG) urethane:

Representative polymerization of segmented polyurethanes containing 20 mol% of bis-MPA-TEMPO and 80 mol% of PEG. In a nitrogen-purged glovebox, a 15 mL vial containing a small magnetic stir-bar was charged with bis-MPA-TEMPO (0.010 g, 0.034 mmol, 0.20 eq.), hexamethylene diisocyanate (HDI) or isophorone diisocyanate (IPDI) (0.167 mmol, 1.00 eq.) and 0.4 mL of dried dichloromethane. The mixture of the reaction was allowed to stir for 15 minutes prior to the addition of the catalyst, DBU (0.002 g, 0.013 mmol). The reaction was monitored by FTIR and once it was reached *c.a.* 50% conversion, PEG diol (0.200 g, 0.133 mmol, 0.80 eq.) was added. The reaction was kept at room temperature for 48 h. When the reaction was completed the catalyst

was quenched with benzoic acid and the polymer was precipitated into cold diethyl ether, isolated by filtration, and dried to obtain an orange solid (yield: 98%-86%).

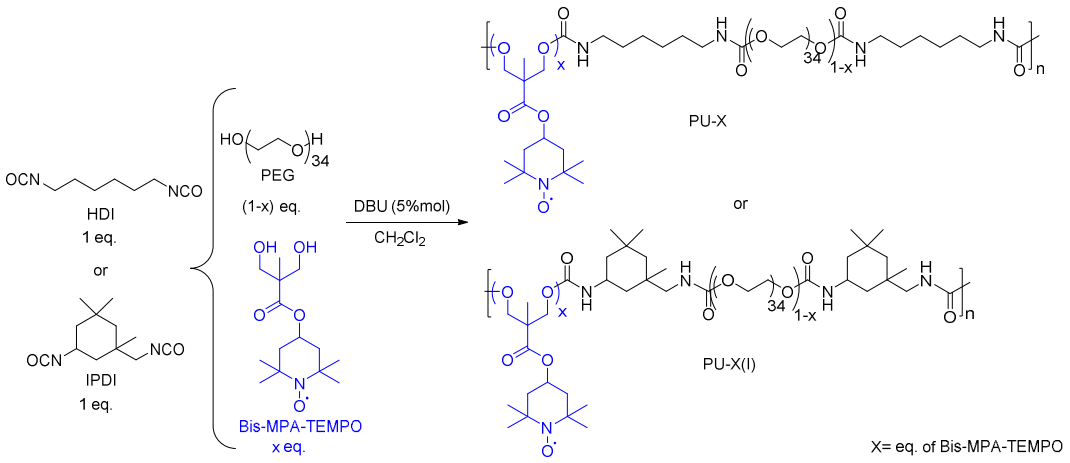

Figure S1 – General synthesis route and molecular structure of the nitroxide-radical containing polyurethane polymers.

Table S1: Composition of the different polymerization reactions between bis-MPA-TEMPO and HDI or IPDI.

Polymer	Diisocyanate	Bis-MPA-TEMPO[a] (eq mol^{-1})	PEG[a] (eq mol^{-1})	PEG segment (wt.%)
PU-0	HDI	0.00	1.00	0.90
PU-5	HDI	0.05	0.95	0.89
PU-10	HDI	0.10	0.90	0.87
PU-15	HDI	0.15	0.85	0.86
PU-20	HDI	0.20	0.80	0.84
PU-30	HDI	0.30	0.70	0.80
PU-40	HDI	0.40	0.60	0.76
PU-50	HDI	0.50	0.50	0.71
PU-20b	IPDI	0.20	0.80	
PU-30b	IPDI	0.30	0.70	
PU-40b	IPDI	0.40	0.60	

[a] Relative to diisocyanate.

A sample of PU-15 was also dissolved in distilled water along with 25 wt% histidine (Sigma, used as received), ultra-sonicated for 10 minutes, dried in an oven at 40 °C for 24 h and finally dried further under vacuum at 50 °C for 68 h.

The weight percentages of crystalline PEO (C_r, wt.%) were calculated using the following equation:

$$C_r = \Delta H_f / \left(w_{PEO} * \Delta H_f^o\right) * 100$$

Where ΔH_f is the enthalpy of fusion (J.g^{-1}) of the crystalline PEO measured by DSC in the PU-X urethanes, w_{PEO} is the weight percentage of PEO segment within the PU-X urethane and ΔH_f^o is the enthalpy of fusion of a fully crystalline PEO (ΔH_f^o = 205 J.g^{-1}).[1–3]

2 - FTIR

The polymerizations were monitored by FTIR. As the reaction proceeded, the characteristic signal of isocyanate stretching at 2265 cm^{-1} decreased and ultimately disappeared. Furthermore, the appearance of two new bands at 1730 and 1550 cm^{-1} assigned to amide I and amide II streching vibrations, confirmed the successful urethane linkage formation. Characterisation data was consistent with previous reports (Garmendia et al., Polym. Chem. 8 (2017) 2693-2701).

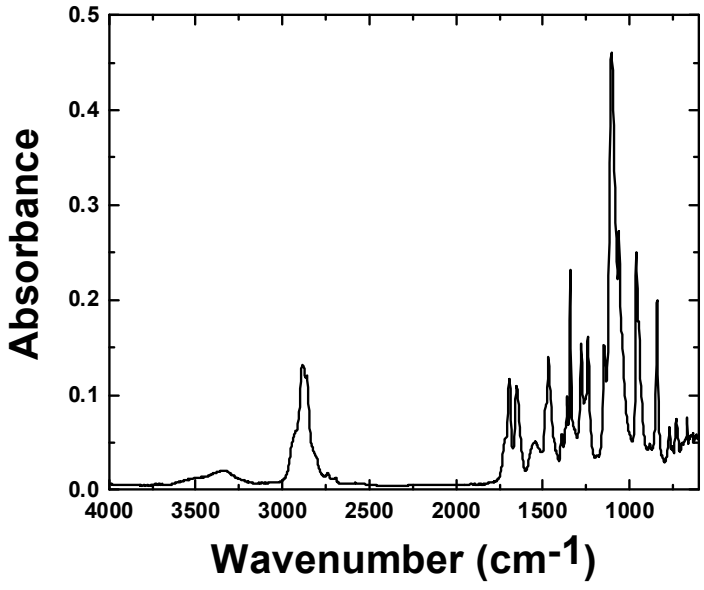

Figure S2 - FTIR spectrum of PU-20.

3 – DSC

Figure S3 shows the DSC traces of PU-X copolymers as a function of TEMPO monomer concentration, up to 15 mol%. Each sample was first quenched from 20 to −100 °C and then heated up to 80 °C at heating rate of 10 °C min^{-1} (first heating scan). This heating cycle was repeated two more times (second and third scans) with the sample cooled from 80 to −100 °C at a rate of 10 °C min^{-1} in between. As a consequence, the first heating scan provides insight into the crystalline nature of the PU-X sample as obtained after synthesis (denoted "PU-X-synthesized"), while the second and third heating scans reveal the crystalline nature of the PU-X sample after crystallization from the melted state (denoted "PU-X-crystallized"). For all samples, the second and third heating scans looked very similar.

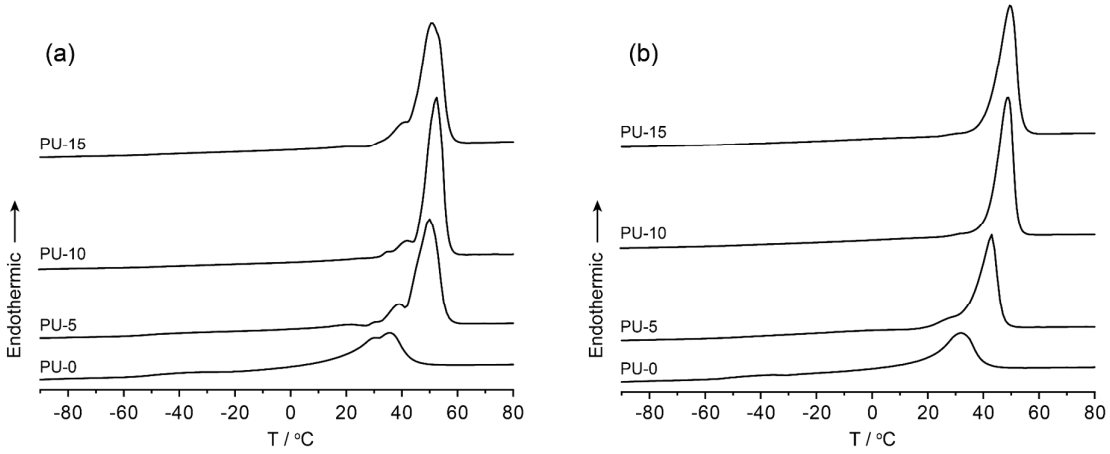

Figure S3 - DSC traces of PU-X as a function of TEMPO monomer concentration. (a) First and (b) second heating scans.

A broad multicomponent endothermic event is observed between 16 and 43 °C for the PU-0-synthesized sample, likely corresponding to the melting of the crystalline PEO chains ($T_{m\ (PEO)}$). The multicomponent nature of melting peak indicates the presence of various PEO crystalline phases with different numbers of folds per molecule.[4] In all samples, this melting transition is sharper and displays a single-component profile in the case of the PU-0-crystallized samples, suggesting that the PEO crystalline phase is more homogenous after quenching from the melt state. As

the TEMPO monomer concentration increases, the melting point of the crystalline PEO is seen to gradually shift to a higher temperature, increasing from 20.8 to 41.6 °C for the PU-0-crystallized and PU-15-crystallized samples respectively. Additionally, the enthalpy of fusion of the crystalline PEO also increases from 69.1 to 125.3 J/g for the PU-0-crystallized and PU-15-crystallized samples respectively. Both of these observations suggest that the incorporation of the TEMPO monomer promotes the crystallization of the PEO chains, and consequently reduces the amount of amorphous PEO in the system. The increase in the crystalline PEO fraction with increasing TEMPO monomer concentration is consistent with the disappearance of the PEO glass transition (visible in Figure S3 at around −50 °C for the PU-0 samples) with increasing TEMPO content. Table S2 summarizes the melting and crystallization temperatures and enthalpies of these PU-X copolymers.

Table S2 - Melting and crystallization temperatures and their respective enthalpies for the PU-X copolymers.

Samples	T_g[a] (°C)	T_C[a,b] (°C)	ΔH_c[b] (j/g_{PEO})	T_m[a,b] (°C)	ΔH_f[b] (j/g_{PEO})	C_r (wt.%)
PU-0-synthesized	-62.0	-	-	16.2	76.7	37.4
PU-0-crystallized	-57.6	-	-	20.8	69.1	33.7
PU-0-quenched	-56.0	-33.5	-32.8	19.0	71.0	34.6
PU-5-synthesized	-56.2	-	-	40.6	121.7	59.4
PU-5-crystallized	-56.2	-	-	33.8	96.7	47.2
PU-5-quenched	-58.5	-44.7	-16.4	31.1	100.9	49.2
PU-10-synthesized	-	-	-	43.1	135.7	66.2
PU-10-crystallized	-	-	-	40.8	114.9	56.1
PU-10-quenched	-	-	-	43.2	116.1	56.6
PU-15-synthesized	-	-	-	45.6	145.0	70.7
PU-15-crystallized	-	-	-	41.6	125.3	61.1
PU-15-quenched	-	-	-	41.4	127.6	62.2

[a] Onset temperature
[b] Extracted from heating scan

Quenching experiments were performed to characterize the effects of fast cooling rates on the crystallization of the PEO segments. Figure S4 shows the DSC traces of PU-X copolymers after quenching from the melt state at a cooling rate of 40 °C min^{-1}. A sharp exothermic event was observed at −33 and −45 °C for the PU-0 and PU-5 samples respectively, corresponding to the crystallization of the PEO segments. The appearance of a crystallization peak suggests the formation of some amorphous

PEO during quenching. However, the incorporation of 5 mol% TEMPO monomer results in a decrease in the enthalpy of crystallization, going from −32.8 to −16.4 J/g, indicating a reduction of the amount of amorphous PEO present in the system. At higher TEMPO monomer concentrations no crystallization peak is observed. These results suggests again that the addition of TEMPO promotes the crystallization of the PEO segments. Table S2 summarizes the melting and crystallization temperature and enthalpy of the PU-X copolymer after quenching (denoted "PU-X-quenched").

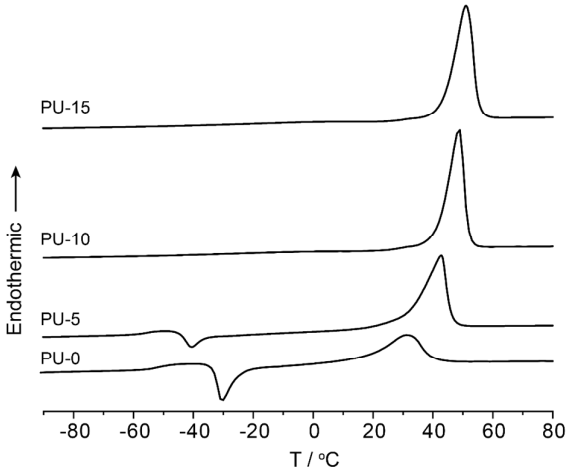

Figure S4 - DSC traces of the PU-X samples after quenching from the melt at a cooling rate of 40 °C min^{-1}.

4 – SAXS & WAXS

WAXS analysis was performed on the polyurethane copolymers to give additional insight on crystallinity of PEO segments and the results is presented in Figure S5b. The PU-O sample exhibits two strong diffraction peaks characteristic of the crystalline PEO,[5,6] which corresponds to a d-spacing of 0.5 and 0.4 nm. Additionally, a broad halo with a d-spacing of ~0.4 nm is also observed for the PU-0 samples, suggesting the presence of amorphous PEO. This is consistent with the DSC data, from which a weight percentage of crystalline PEO of 33.7 % were extrapolated for the PU-0 sample. Again, the introduction of TEMPO monomer into the polyurethane chains results in the disappearance of this broad diffraction halo, suggesting a reduction of extent of amorphous PEO present. Interestingly, the extent of amorphous PEO increase again, when a TEMPO concentration of 40 and 50 mol% is used, as suggested by the presence of a low intensity diffraction halo (d-spacing of ~ 0.4 nm). This is consistent with the sudden increase in the spatial periodicity associated with the macrophase separation, suggesting the formation of a less dense PEO and/or TEMPO phase. It is likely that the reduction of the PEO and/or TEMPO confinement reduces the amount of crystalline PEO. Additionally, this phenomenon is likely to be the cause of the disruption of the local medium range observed at lower TEMPO concentration. Table S3 summarizes the spatial periodicity of the diffraction peaks observed for the PU-X copolymers as well as the phase assignment and lattice parameter.

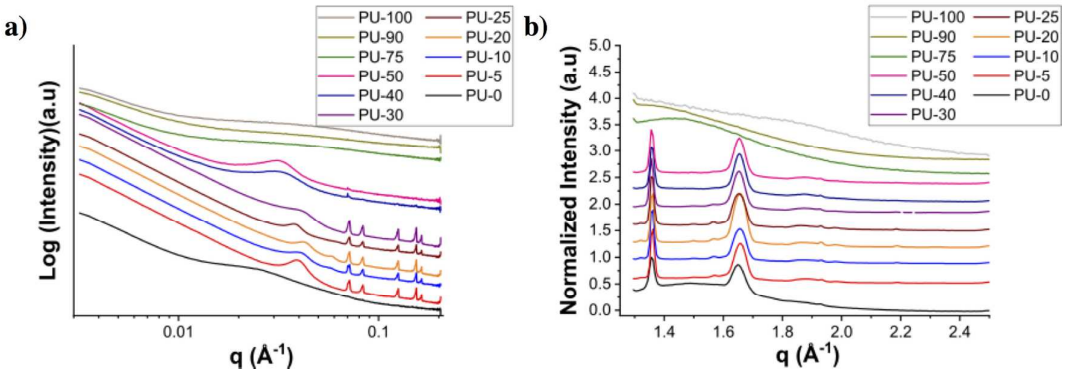

Figure S5 – Room-temperature (a) SAXS and (b) WAXS patterns of the polyurethanes as a function of TEMPO concentration, up to 100 mol% TEMPO.

Table S3 – Diffraction peak positions, phase assignment and their respective lattice parameter for the PU-X copolymers.

Sample Name	Peak position (theoretical values) ($Å^{-1}$)	Phase assignment	Lattice parameter (nm)
PU-0	0.023	Weakly microphase separated	27.5
PU-5	0.039	Lamellar phase	16.1
	0.072 0.084 0.126 0.155 0.164	Local medium range order	Unknown
PU-10	0.039 0.058 (0.056)	Bicontinuous /discontinuous cubic phase ($Im\bar{3}m$)	22.0 ± 0.5
	0.072 0.084 0.126 0.155 0.164	Local medium range order	Unknown
PU-20	0.041 0.058 (0.058)	Bicontinuous /discontinuous cubic phase ($Im\bar{3}m$)	21.8 ± 0.3
	0.072 0.084 0.126 0.155 0.164	Local medium range order	Unknown
PU-25	0.038	Lamellar phase	16.7
	0.072 0.084 0.126 0.155 0.164	Local medium range order	Unknown
PU-30	0.041	Lamellar phase	15.3
	0.072 0.084 0.126 0.155 0.164	Local medium range order	Unknown
PU-40	0.033	Lamellar phase	19.0
PU-50	0.032	Lamellar phase	19.9
PU-75	0.039	Weakly microphase separated	15.9
PU-90	0.039	Weakly microphase separated	15.9
PU-100	0.038	Weakly microphase separated	16.7

5 - DFT

Carbon	σ_{iso} / ppm	δ_{iso} / ppm
1	96.37	72.1
2	96.80	72.0
3	94.73	73.4
4	97.04	71.6
5	95.09	73.0
6	97.21	71.6
7	95.29	73.0
8	95.44	72.7
9	95.80	72.3
10	95.21	73.0
11	95.39	72.9
12	94.97	73.1
13	93.17	74.7
14	95.47	72.7

Table S4 - Calculated ^{13}C isotropic chemical shielding values (σ_{iso}) for the 14 distinct carbon sites in the PEO crystal structure after DFT optimisation of the atomic positions. Also shown are isotropic chemical shifts (δ_{iso}) reported in D.J. Harris et al., Polymer 46 (2005) 11737-11743, assigned based on a linear correlation. We note that these assignments differ from that of Harris et al. and are based solely on the best correlation with our calculated σ_{iso} values (Figure S4).

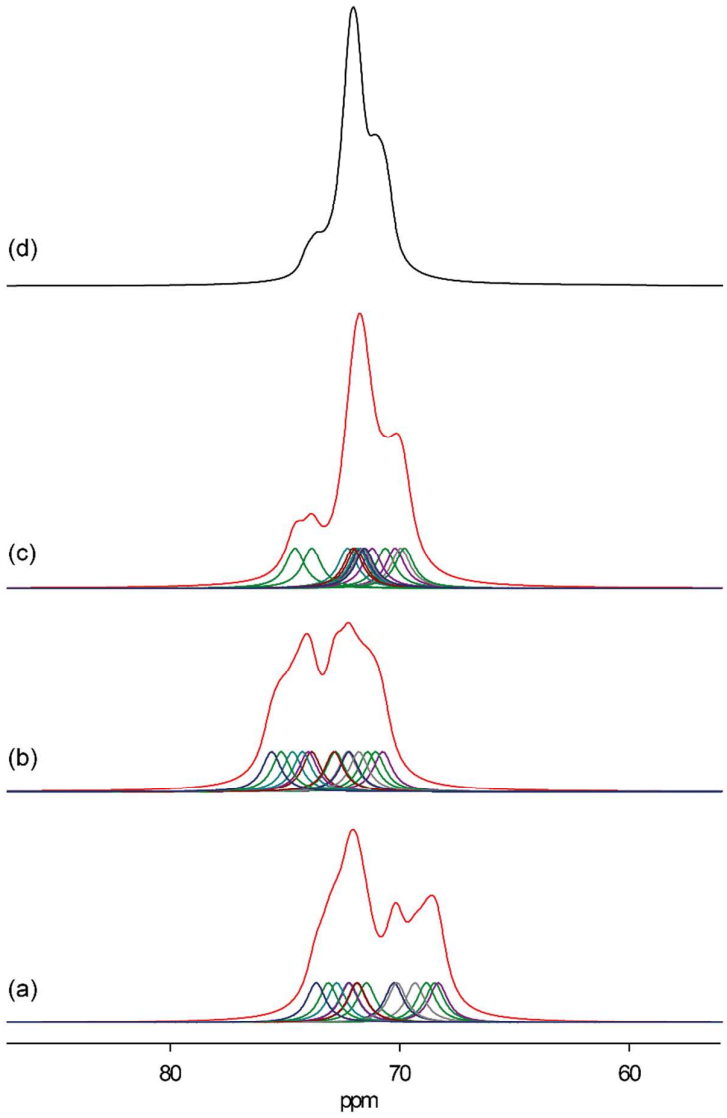

Figure S6 - ^{13}C NMR spectra as predicted using DFT calculations based on (a) the unoptimised crystal structure, (b) the crystal structure with H atom positions optimised and (c) the crystal structure with all atomic positions optimised (cell dimensions fixed). Red traces show the net spectra with the individual peaks also shown beneath. (d) The experimental DNP-enhanced ^{13}C CPMAS spectrum or PU-15, expanded about the PEO region.

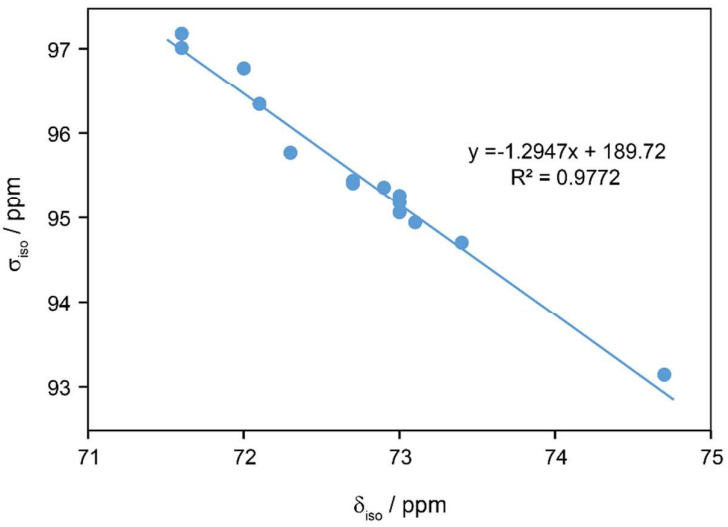

Figure S7 - Correlation of isotropic chemical shielding values (σ_{iso}) calculated form the DFT-optimised crystal structure with experimental isotropic chemical shifts (δ_{iso}) reported in D.J. Harris et al., Polymer 46 (2005) 11737-11743.

6 - DFT-optimised PEO crystal structure

Space group: P21/A (14)

Cell dimensions: a = 8.05 Å, b = 13.04 Å, c = 19.48 Å, α = 90°, β = 125.4°, γ = 90°

Fractional atomic coordinates:

	X	Y	Z
O1	0.0765	0.35951	-0.04235
C1	-0.05207	0.31131	-0.02388
C2	0.07673	0.24666	0.05409
O2	0.20018	0.31153	0.12516
C3	0.3426	0.25471	0.19889
C4	0.4655	0.32609	0.27274
O3	0.33712	0.36976	0.29303
C5	0.44474	0.4383	0.36237
C6	0.30047	0.48372	0.37969
O4	0.24019	0.40679	0.4129
C7	0.08202	0.44164	0.4192
C8	0.03832	0.3607	0.46188
O5	0.19427	0.36102	0.54993
C9	0.17823	0.27534	0.59089
C10	0.33135	0.28531	0.68477
O6	0.26363	0.36021	0.71667
C11	0.41426	0.37908	0.80352
C12	0.33818	0.45617	0.8369
O7	0.18743	0.41132	0.84356
C13	0.11528	0.48186	0.87652
C14	-0.03141	0.429	-0.11092
H1	-0.13491	0.37016	-0.01358
H2	-0.16613	0.26146	-0.07628
H3	-0.02412	0.19836	0.06197
H4	0.17408	0.19505	0.04639
H5	0.26221	0.19842	0.21257
H6	0.44789	0.21158	0.19048
H7	0.59066	0.28153	0.32636
H8	0.53423	0.38744	0.25731
H9	0.56886	0.39716	0.41918
H10	0.51649	0.50077	0.34967
H11	0.37941	0.54707	0.42543
H12	0.16552	0.51615	0.32106
H13	0.12614	0.51406	0.45537
H14	-0.05792	0.45821	0.35609
H15	-0.1112	0.37644	0.45012
H16	0.02778	0.28471	0.43436
H17	0.0225	0.26906	0.57496
H18	0.20844	0.20372	0.56941
H19	0.3526	0.21025	0.71533
H20	0.48133	0.30721	0.69913
H21	0.45767	0.30707	0.84018
H22	0.55332	0.41038	0.81254
H23	0.4691	0.48313	0.89942
H24	0.27574	0.52397	0.79491
H25	0.2451	0.51276	0.93757
H26	0.03589	0.54696	0.83298
H27	-0.14831	0.38793	-0.16944
H28	-0.11005	0.48807	-0.09871

7 - PEO domain size measurement

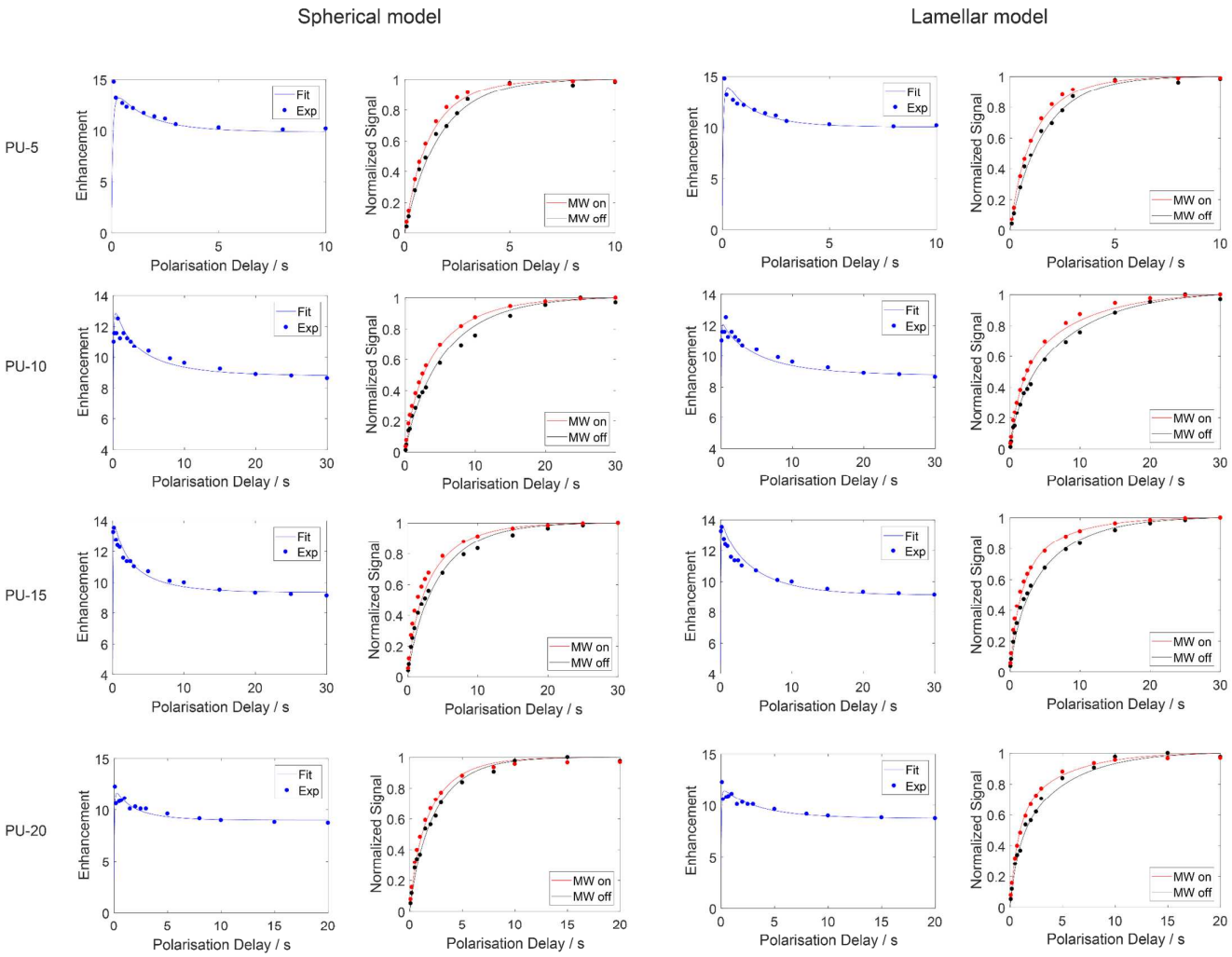

Figure S8 - Fits of the DNP data to a spin-diffusion based model. Typical parameters used: $T_{1,source}$ = 40 ms, $T_{1,target}$ = 10 s, D_{target} = D_{source} = 1 × 10^{-5} μm^2s^{-1} and ε_0 = 25. These parameters, along with L_{target} and L_{source}, were based on those used in A.C. Pinon et al., J. Phys. Chem. C 121 (2017) 15993-16005 and were manually varied to achieve the best fit. See this reference and related materials for a detailed description of the model and definitions of these parameters.

8 - Comparison of different linker groups

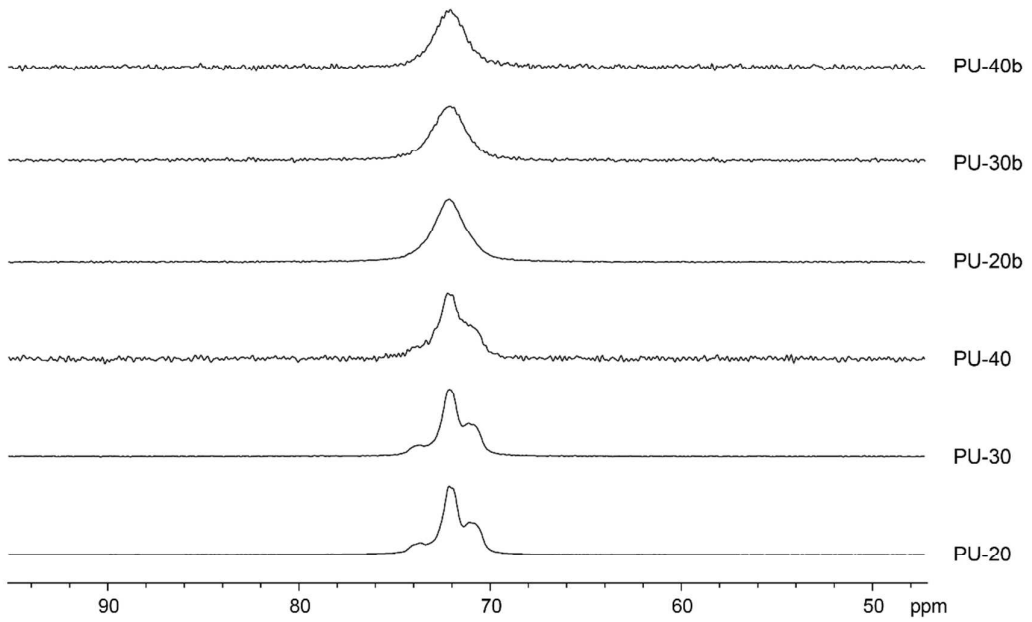

Figure S9 - DNP-enhanced ^{13}C CPMAS spectra obtained from the polymer samples prepared as shown in Table S1 (PU-20, PU-30 and PU-40 with HDI linkers, PU-20b, PU-30b and PU-40b with bulkier IPDI linkers). The latter samples show significant broadening of the PEO ^{13}C NMR signals, indicating a much more disordered structure.

9 - References

(1) Shieh, Y. T.; Liu, G. L.; Hwang, K. C.; Chen, C. C. Crystallization, Melting and Morphology of PEO in PEO/MWNT-g-PMMA Blends. Polymer. 2005, 46, 10945–10951.

(2) Sanchez-Soto, P. J.; Gines, J. M.; Arias, M. J.; Novak, C.; Ruiz-Conde, A. Effect of Molecular Massa on the Melting Temperature , Enthalpy and Entropy of Hydroxi-Terminated PEO. J. Therm. Anal. Calorim. 2002, 67, 189–197.

(3) Martuscelli, E.; Silvestre, C.; Addonizio, M. L.; Amelino, L. Phase Structure and Compatibility Studies in Poly(Ethylene Oxide)/Poly(Methyl Methacrylate) Blends. Die Makromol. Chemie 1986, 187 (6), 1557–1571.

(4) Cheng, S. Z. D.; Wunderlich, B. Molecular Segregation and Nucleation of Poly (Ethylene Oxide) Crystallized from the Melt . II . Kinetic Study. J. Polym. Sci. Part B Polym. Phys. 1986, 24, 595–617.

(5) Zhu, L.; Mimnaugh, B.; Ge, Q.; Quirk, R.; Cheng, S. Hard and Soft Confinement Effects on Polymer Crystallization in Microphase Separated Cylinder-Forming PEO- b-PS/PS Blends. Polymer. 2001, 42, 9121–9131.

(6) Zhu, L.; Cheng, S. Z. D.; Calhoun, B. H.; Ge, Q.; Quirk, R. P.; Thomas, E. L.; Hsiao, B. S.; Yeh, F.; Lotz, B. Phase Structures and Morphologies Determined by Self-Organization , Vitrification , and Crystallization : Confined Crystallization in an Ordered Lamellar Phase of PEO- b -PS Diblock Copolymer. Polymer. 2001, 42, 5829–5839.